Preprints of the 19th World Congress
The International Federation of Automatic Control
Cape Town, South Africa. August 24-29, 2014

Advanced EIS Techniques for Performance Evaluation of Li-ion Cells

**T. Stockley*, K. Thanapalan, M. Bowkett,
J. Williams, M. Hathway**

**Centre for Automotive and Power Systems Engineering (CAPSE), University of South Wales, United Kingdom, CF371DL (Tel: 01443482542; e-mail:thomas.stockley@southwales.ac.uk).*

Abstract: This paper provides an advanced electrochemical impedance spectroscopy (EIS) technique for improving the state of charge and state of health estimation of Li-ion cells. This advanced technique is derived from various tests and experimental studies conducted in the CAPSE labs at the University of South Wales. The results indicate that the technique is very accurate compared to other methods such as coulomb counting and OCV prediction method.

1. INTRODUCTION

Lithium cells have played an increasingly key role in the automotive and power systems sectors in recent years. They offer benefits of high cell voltage, high energy density, high cycle count and low self discharge rate when compared to alternative technologies (Chen et al. 2012; Weinert et al. 2007; Suzuki et al. 2003 and Ng et al. 2005). However, the fact that the cells require constant monitoring and management currently limits the extent of their application in both of these industries. Monitoring the cells is vital to ensure that they are used within safe operating limits (Lu et al. 2013), and management enables maximum performance and cell balancing (Roscher et al. 2012; Bowkett et al. 2013). The monitoring and management is usually conducted by a battery management system (BMS) (Cheng et al. 2011).

As well as temperature, voltage and current logging, the BMS performs two complicated functions: 1) Estimation of how much of the battery energy has been consumed by the application, known as the state of charge (SoC). 2) Estimation of how much of the battery life has been reduced throughout the life of the application, known as the state of health (SoH). These are the more complicated BMS functions because they involve calculation, which can range from simple mathematics to real time system modelling, depending on the function technique and level of accuracy required (Bowkett et al. 2013, Kim and Cho 2013). However, the determination and maintenance of SoC and SoH is very important in order to evaluate the cell performance and possible performance improvements (Hussein and Batarseh 2011).

Three types of SoC estimation techniques are currently being used. These are: 1) Coulomb counting. 2) Open circuit voltage/state of charge (OCV/SoC) lookup table. 3) Electrochemical impedance spectroscopy (EIS) techniques. There is an alternative modelling method to the EIS technique, known as electrochemical modelling, which uses complex mathematical equations for the prediction of SoC and SoH. This method has not been explored further in this paper due to the very high computational requirement and the fact that it is not as accurate as equivalent circuit modelling, which is a product of the EIS technique (He et al. 2012).

Coulomb counting, as the name suggests, involves monitoring and counting the current that has entered or left the cell (Ng et al. 2009). Although it is the most commonly used method for SoC estimation, due to its low implementation time, it can be susceptible to measurement errors. Errors occur due to accumulation errors and problems with initial SoC measurements (Cho et al. 2012).

A slightly more complicated but more accurate technique is the measurement of the open circuit voltage (OCV) and comparison to a predefined lookup table to estimate the SoC. This technique has a major flaw in the fact that the OCV can only be accurately measured at an equilibrated state which can take between 2 to 6 hours. Therefore, the OCV cannot be calculated during use (Aylor et al. 1992). Recent research work shows that this open circuit period may be reduced and the technique become more viable (Stockley et al. 2013).

Although the EIS technique is difficult to implement and has a high computer requirement the equivalent circuits that can be designed from its results are superior in accuracy to alternative technologies (Hu et al. 2012). EIS equipment uses an AC voltage waveform, with a known amplitude, to excite the cell and measure the responding current wave. The impedance of the cell can be calculated from the voltage and current waveforms and plotted on a Nyquist plot for analysis (Macdonald 2012). The Nyquist plot provides sufficient information to estimate the state of several battery components, which imply the SoC and SoH of the cell on test.

This technique is very accurate and as mentioned above can be used to calculate both the SoC and the SoH of the cell (Salkind et al. 1999). However, although work has been carried out to perform measurements under load condition

(Jespersen et al. 2009), the EIS method may suffer from the need to be conducted at an equilibrated state (Gamry Instruments 2010). Despite this disadvantage, the EIS technique is being researched for use in practical systems, see for example, (Salkind et al. 1999; Blanke et al. 2005; Singh et al. 2006; Eddahech et al. 2012). Salkind et al. 1999 have performed work on the EIS technique for primary lithium cells and secondary NiMH cells, to estimate both the SoC and SoH. Blanke (Blanke et al. 2005) uses the EIS method on lead acid cells to determine the SoC, SoH and available cranking power of a battery bank for HEV applications. The author explains that by using EIS, the remaining power can be calculated regardless of cell temperature and state of charge. Singh et al (Singh et al. 2006) have used a combination of EIS and fuzzy logic to produce two models for SoC and SoH of small lithium batteries. The model parameters in this case have been obtained from a duty cycle for portable defibrillators, proving that EIS can be used in many applications. Eddahech et al. (Eddahech et al. 2012) explain that one of the biggest contributors to SoH deterioration is the storage (non use) conditions of lithium cells. The authors have identified that the solution resistance of a cell increases with age and have, therefore, produced an equation, which can provide the remaining useful life (RUL) of the cell. This equation describes the functionality of the solution resistance, temperature and SoC.

This paper is organised as follows. Section 2 provides a brief overview of the EIS technique and section 3 uses an equivalent circuit to explain the effect of temperature, SoC and SoH on a Lithium Manganese Nickel Cobalt Oxide ($LiMNCO_2$) cell. Finally, the SoH estimation techniques and a brief conclusion to this work are presented.

2. EIS METHODOLOGY

EIS is a highly accurate method for the determination of SoC and SoH of battery systems. Due to its higher accuracy when compared to alternate methods, and the fact that the EIS method allows determination of both the SoC and the SoH by one test containing an AC frequency sweep, the EIS method was chosen for this work and further work to be completed at a later date. The EIS method works by measuring the impedance of the cell through a range of AC signals at varying frequency (Haiying et al. 2011). The measured impedance can be displayed in a Nyquist plot as seen in Figure 1.

Because the electrochemical cell contains both inductive and capacitive characteristics the impedance result of an AC excitation voltage will be a complex number. This means that the current and voltage waveforms will be at a phase difference and, therefore, provide a phase angle as well as magnitude. The wide frequency span of the AC signals applied to the cell means that each individual component can be studied, as the different components are affected in different ways to each of the individual frequencies. Because a pure resistance has no phase change, a measurement point on the X axis (real impedance) represents a purely resistive impedance. A measurement point above the X axis shows that there is a capacitive element to the impedance, characterised by a phase shift angle of -1 to -90°. A measurement point below the X axis shows that there is an inductive element to the impedance, characterised by a phase shift angle of 1 to 90°. This can be seen in Figure 1, and is further highlighted by the red arrows to show the resistive, capacitive and inductive characteristics.

As the impedance measurement from the whole test frequency spectrum is provided on the Nyquist plot, the individual parameters required for the equivalent circuit model can be estimated. These parameters represent the series resistance (R_s) caused by the terminals and measurement cables, the charge transfer resistance (R_{CT}) caused from polarising the electrons, the double layer capacitance (C_{DL}) caused by a small insulating layer between the electrode and the electrolyte, diffusion capacitance (C_{diff}), and the cells' inductance (L). Although the actual frequency measurements cannot be attained from the Nyquist plot alone, the frequency ranges from high (kHz) to low (mHz) as the plot is observed from left to right.

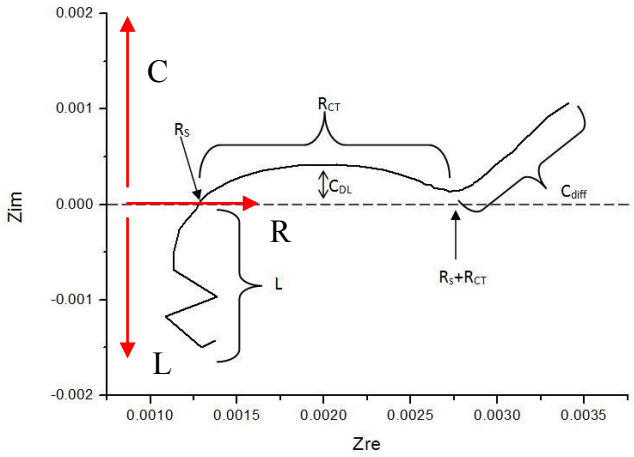

Figure 1: Nyquist plot breakdown for equivalent circuit model

The parameters from Figure 1 can be used to create an equivalent circuit model as seen in Figure 2. By using the equivalent circuit model, the change in parameters as the cell conditions vary can be observed. Figure 2 illustrates use of a constant phase element instead of the capacitor, and a Warburg impedance component to represent the diffusion element (C_{diff}) at low frequencies. The constant phase element allows a non-ideal capacitor (the double layer capacitance) to be modelled by the use of a phase compensation value. The phase compensation value causes the suppression in the semi-circle as can be seen in Figure 1. The Warburg impedance is a circuit element that can accurately represent the diffusion in an electrochemical cell. By using the circuit in Figure 2, the Nyquist plot in Figure 1 could be accurately simulated.

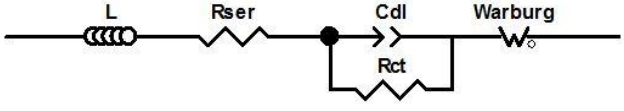

Figure 2: Equivalent circuit model from first principles

As mentioned above, by using the equivalent circuit the parameters that change due to various cell conditions can be obtained. For example, Figure 3 shows that the series resistance increases as the temperature decreases. To obtain the results of the EIS tests a frequency response analyser (FRA) was used. By using the FRA equipment, an industrial battery tester and an environmental chamber the required cell conditions were created for testing. The test setup has been provided in a block diagram in Figure 4. The industrial battery tester was used for SoC adjustment prior to the EIS measurement. The cell on test can be seen in the photograph in Figure 5.

The principles of the EIS technique and analysis of the results will allow a control system to be designed and implemented onto a microcontroller, which can be used in a functioning battery management system (BMS). The next section of this paper will explain the results achieved from the testing phase and provide the equivalent circuit model for the use of EIS analysis.

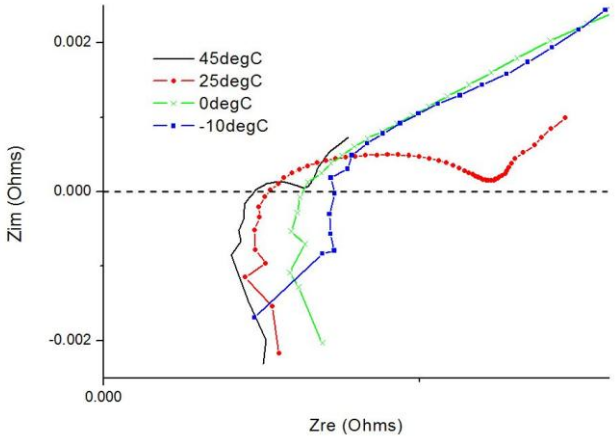

Figure 3: Comparison of EIS results at a range of cell temperatures.

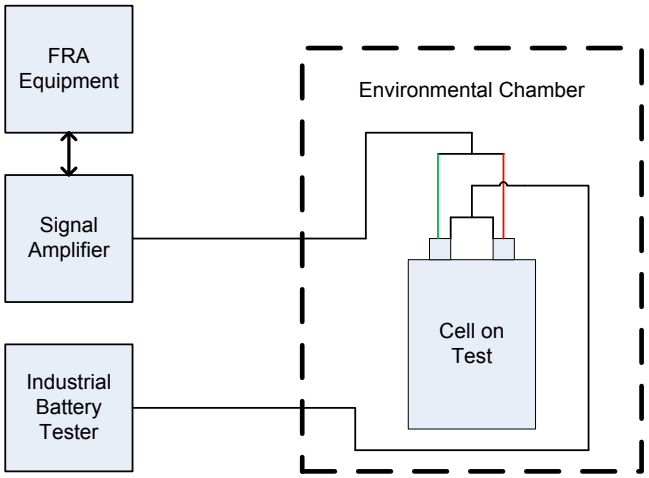

Figure 4: Block diagram of test setup

3. EXPERIMENTAL STUDY

Testing was carried out at various temperatures, SoC and SoH to gain a good understanding of the cell characteristics. Figure 6 provides the impedance response of the $LiNMCO_2$ cell at 80% SoC, 100% SoH and 25°C. The tests were carried out for a frequency span of 10kHz to 10mHz.

By using electrochemical analysis software, and the principles shown in Figure 1, the EIS response in Figure 6 was modelled as the equivalent circuit shown in Figure 7.

Figure 5: $LiNMCO_2$ cell on EIS test

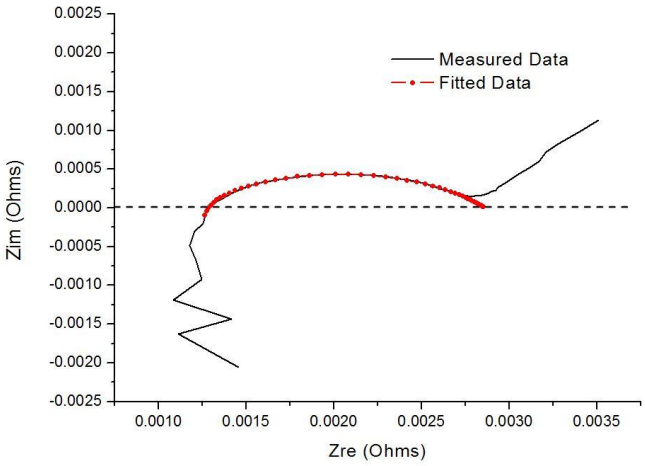

Figure 6:Measured data and fitted simulation for an 80% SoC, 100% SoH and 25°C EIS test

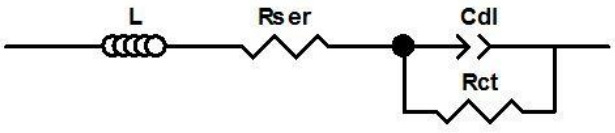

Figure 7:Simple equivalent circuit for SoC and SoH estimation

In this paper, the use of the Nyquist plot to estimate the SoC and SoH of the cell is investigated. From Figure 6 it can be seen that the only areas that have been modelled are the large semi circle (RC component) and the crossing at the x axis (series resistance). This is because it is possible that both the SoC and SoH can be estimated from this semi-circle. As it can be seen in Figure 3, the series resistance increases with

temperature reduction and health deterioration as expected from Figure 11. Figure 8 shows that the RC circle increases as SoC decreases, giving possibility to SoC estimation from parameter R_S+R_{CT} in Figure 1. The inductive element (measurements below the x axis) and the diffusion element (C_{diff} in Figure 1) has been disregarded in this study. This is because the inductive element is understood to be an inductance caused by the measurement cables (Zhang et al. 2013), and the diffusion element is only present at very low frequencies. The low frequencies are too time consuming for a BMS in a real world system.

To achieve the fitted data result in Figure 6, the following equivalent circuit parameters were applied. L=7nH, R_{ser}=1.2mΩ, C_{dl}=8.4F with a phase compensation of 0.6132 and R_{CT}=0.00166mΩ. This paper will further show how the circuit components change with the condition of the cell and how this knowledge can be used by a real world BMS.

3.1 SoC effect on equivalent circuit model

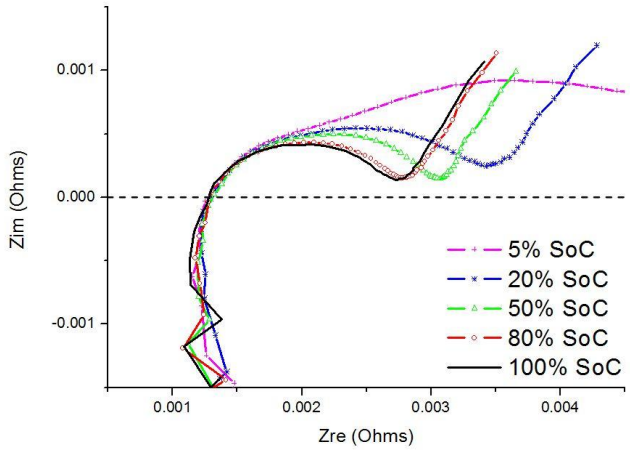

Figure 8: Comparison of EIS response at various SoC

Figure 8 shows that as the SoC decreases the imaginary impedance increases. By fitting the simple model in Figure 7 to each of the responses in Figure 8, the changing parameters may be monitored. It should be noted that the series resistance changes very little throughout the full SoC range, as is expected. The four Nyquist plots in Figure 9 show that the fitted results from the equivalent circuit in Figure 7 is an accurate representation of the cell at the varying SoC range. The 5% SoC plot was not included because as Shim and Striebel (Shim and Striebel 2003) conclude, a lithium cell should not be used below 20% SoC, or cycle life may be dramatically reduced. Table 1 has been constructed to provide the reader with the component parameters used for Figure 9, so that a better insight of the proposed EIS methodology may be gained.

Table 1 shows that the charge transfer resistance changes greatly with the cell's SoC, however, the other parameters stay relatively constant. This shows that the charge transfer resistance is the primary component in the increased impedance of a cell as the SoC declines. Figure 10 shows the charge transfer resistance against SoC, showing the possibility of using R_{CT} for SoC estimations for this battery technology.

Table 1. Equivalent Circuit Parameters vs SoC

SoC	L (H)	R_{ser} (Ω)	C_{dl} (F)	C_{dl} Phase	R_{CT} (Ω)
100%	7x10-9	0.00119	18.4	0.6132	0.001605
80%	7x10-9	0.0012	18.4	0.6132	0.00166
50%	7x10-9	0.001229	18.4	0.625	0.0019
20%	7x10-9	0.00116	18.4	0.655	0.00244

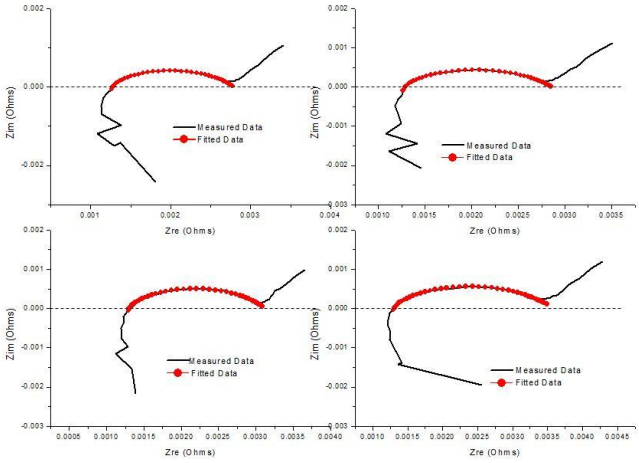

Figure 9: Measured and fitted Nyquist plots for 100%, 80%, 50% and 20% SoC at 25°C

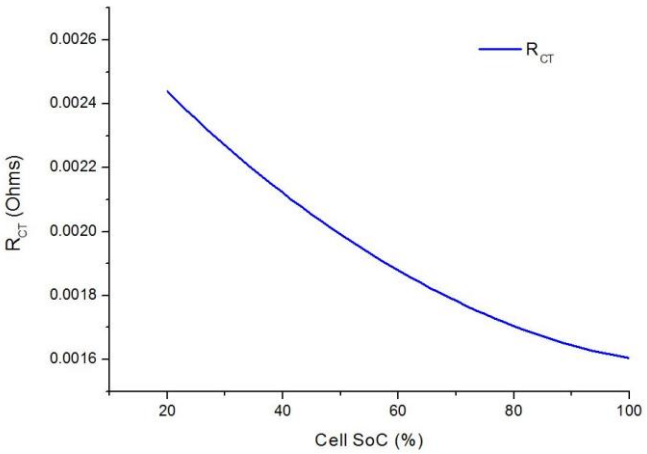

Figure 10: Charge transfer resistance vs SoC

3.2 SoH effect on equivalent circuit model

In the case of the SoH analysis, initial investigations indicated that the EIS results will show a clear variation in the series resistance component as the cell changes SoH. This investigation is based upon a separate test that is being carried out at the Centre for Automotive and Power Systems Engineering (CAPSE) labs, which monitors the cell

characteristics through an automotive life cycle test. The test performs set cycles repeatedly, stopping once a week for characterisation specific tests. From the characteristic specific tests the DC resistance of the cell can be calculated. Table 2 shows the DC resistance results for the cells from 100% to 50% SoH. The SoH was calculated from 1C capacity tests.

Table 2 - SoH vs DC resistance for lithium cell

SoH (%)	DC Resistance (mΩ)
100	2
98.1	2.1
89.15	2.3
79.1	2.4
69.35	2.7
56.25	4

The change in series resistance with SoH has been identified by previous research work, see for example (Eddahech et al. 2012), which monitors the SoH characteristics when different storage methods are applied. The results in Table 2 show that there is a significant change in series resistance as the SoH decreases from 100% to 50% SoH. A DC resistance of more than 4mΩ is unlikely to be seen in a practical system, however, as most applications would replace the battery prior to 50% SoC. This is due to poor capacity and poor charge/discharge efficiencies past this point.

Using the information in Table 2, the series resistance values have been estimated for the $LiNMCO_2$ cell and the results are shown in Figure 11.

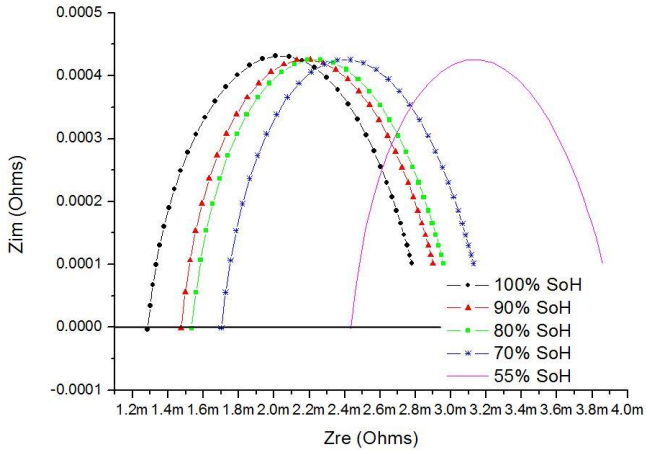

Figure 11: Estimated Nyquist plots for varying SoH

3.3. Temperature effect on equivalent circuit model

By considering the niquist plot in Figure 3 it can be seen how an unstable temperature can alter both the SoC and SoH measurement readings. The first effect is an increase in the series resistance of the cell as the temperature decreases, which could provide an inaccurate reading for the SoH. The second effect is that the RC element increases as the temperature decreases, which would alter the SoC measurement. This can be clearly seen by comparing the plot at 45°C and -10°C, where the RC element changes from a semi circle to a 45° straight line, similar to a diffusion element.

4. DISCUSSION AND CONCLUDING REMARK

From the results and the analysis presented in this paper, in particular in section 3, the EIS method is a viable technique for the estimation of SoC and SoH of $LiNMCO_2$ cells. But it is important to note that the technique is not without flaws, as is proven by the work in section 3C, which shows that the temperature greatly affects the SoC and SoH readings. Furthermore, from the analysis of the results it is seen that the SoC, SoH or temperature of the cell can be obtained from the EIS results when two of the other parameters are known.

In a working BMS it is likely that the temperature is a known parameter from the use of carefully placed thermocouples, which means that the SoC and SoH can be calculated from the equivalent circuit values. It is likely that the SoH will only be measured when the cell is fully charged or discharged so that the SoC is at a known state. The SoH can then be used as a known constant in the calculation of the SoC. A performance map needs to be created for the EIS method to work. The performance map will allow the predefined circuit element values for the full range of temperature, SoC and SoH, and is currently being implemented as part of the overall research scope at the CAPSE labs.

5. ACKNOWLEDGEMENTS

The first author would like to acknowledge the financial support from Knowledge Economy Skills Scholarships (KESS), Remote Utility Monitoring and Management (RUMM) Ltd. and the University of South Wales during this research project. The authors would also like to thank the staff of the Centre for Automotive and Power Systems Engineering (CAPSE) for their assistance.

6. REFERENCES

Aylor, J.H., Thieme, A. & Johnson, B.W., 1992. A battery state-of-charge indicator for electric wheelchairs. *IEEE Transactions on Industrial Electronics*, 39(5), pp.398 –409.

Blanke, H. et al., 2005. Impedance measurements on lead–acid batteries for state-of-charge, state-of-health and cranking capability prognosis in electric and hybrid electric vehicles. *Journal of Power Sources*, 144(2), pp.418–425.

Bowkett, M. et al., 2013. Design and implementation of an optimal battery management system for hybrid electric vehicles. In *2013 19th International Conference on Automation and Computing (ICAC)*. 2013 19th International Conference on Automation and Computing (ICAC). pp. 1–5.

Cheng, K.W.E. et al., 2011. Battery-Management System (BMS) and SOC Development for Electrical Vehicles. *IEEE Transactions on Vehicular Technology*, 60(1), pp.76–88.

Cho, S. et al., 2012. State-of-charge estimation for lithium-ion batteries under various operating conditions using an equivalent circuit model. *Computers & Chemical Engineering*, 41, pp.1–9.

Eddahech, A. et al., 2012. Behavior and state-of-health monitoring of Li-ion batteries using impedance spectroscopy and recurrent neural networks. *International Journal of Electrical Power & Energy Systems*, 42(1), pp.487–494.

Gamry Instruments, 2010. Basics of Electrochemical Impedance Spectroscopy: Application Note. Available at: http://www.gamry.com/application-notes/basics-of-electrochemical-impedance-spectroscopy/ [Accessed November 15, 2013].

Haiying, W. et al., 2011. Study on correlation with SOH and EIS model of Li-ion battery. In *2011 6th International Forum on Strategic Technology (IFOST)*. 2011 6th International Forum on Strategic Technology (IFOST). pp. 261–264.

He, H. et al., 2012. Comparison study on the battery models used for the energy management of batteries in electric vehicles. *Energy Conversion and Management*, 64, pp.113–121.

Hu, X., Li, S. & Peng, H., 2012. A comparative study of equivalent circuit models for Li-ion batteries. *Journal of Power Sources*, 198, pp.359–367.

Hussein, H.A.-H. & Batarseh, I., 2011. An overview of generic battery models. In *2011 IEEE Power and Energy Society General Meeting*. 2011 IEEE Power and Energy Society General Meeting. pp. 1–6.

Jespersen et al., 2009. Capacity Measurements of Li-Ion Batteries using AC Impedance Spectroscopy. *World Electric Vehicle Journal,* 3(24)

Kim, J. & Cho, B.H., 2013. Pattern Recognition for Temperature-Dependent State-of-Charge/Capacity Estimation of a Li-ion Cell. *IEEE Transactions on Energy Conversion*, 28(1), pp.1–11.

Lu, L. et al., 2013. A review on the key issues for lithium-ion battery management in electric vehicles. *Journal of Power Sources*, 226, pp.272–288.

Macdonald, J.R., Scientific Publications of James Ross Macdonald-temporally ordered. Available at: http://www.jrossmacdonald.com/jrmpub.html [Accessed November 15, 2013].

Ng, K.S. et al., 2009. Enhanced coulomb counting method for estimating state-of-charge and state-of-health of lithium-ion batteries. *Applied Energy*, 86(9), pp.1506–1511.

Ng, P.K., Mathiesen, G. & Davis, R., 2005. System Integration of Lithium-Ion battery in Telecommunication Back-up Power Plant. In *Telecommunications Conference, 2005. INTELEC '05. Twenty-Seventh International*. Telecommunications Conference, 2005. INTELEC '05. Twenty-Seventh International. pp. 205–210.

Roscher, M.A., Leidholdt, W. & Trepte, J., 2012. High efficiency energy management in BEV applications. *International Journal of Electrical Power & Energy Systems*, 37(1), pp.126–130.

Salkind, A.J. et al., 1999. Determination of state-of-charge and state-of-health of batteries by fuzzy logic methodology. *Journal of Power Sources*, 80(1–2), pp.293–300.

Shim, J. & Striebel, K.A., 2003. Characterization of high-power lithium-ion cells during constant current cycling: Part I. Cycle performance and electrochemical diagnostics. *Journal of Power Sources*, 122(2), pp.188–194.

Singh, P. et al., 2006. Fuzzy logic modeling of EIS measurements on lithium-ion batteries. *Electrochimica Acta*, 51(8–9), pp.1673–1679.

Stockley, T. et al., 2013. Development of an OCV prediction mechanism for lithium-ion battery system. In *2013 19th International Conference on Automation and Computing (ICAC)*. 2013 19th International Conference on Automation and Computing (ICAC). pp. 1–6.

Suzuki, I., Shizuki, T. & Nishiyama, K., 2003. High power and long life lithium-ion battery for backup power sources. In *Telecommunications Energy Conference, 2003. INTELEC '03. The 25th International*. Telecommunications Energy Conference, 2003. INTELEC '03. The 25th International. pp. 317–322.

Weinert, J.X., Burke, A.F. & Wei, X., 2007. Lead-acid and lithium-ion batteries for the Chinese electric bike market and implications on future technology advancement. *Journal of Power Sources*, 172(2), pp.938–945.

Zhang, L., Liu, F. & Anil V, V., 2013. Electrochemical Impedance Spectroscopy of Gadolina-Doped Ceria: Role of Leads/Instrument Impedance. *Meeting Abstracts*, MA2013-02(11), pp.789–789.